

# The First MAXI/GSC Catalog in the Extragalactic Sky

K.Hiroi,<sup>1</sup> Y.Ueda,<sup>1</sup> N.Isobe,<sup>1</sup> M.Hayashida,<sup>1</sup> and MAXI team

<sup>1</sup> Department of Astronomy, Kyoto University  
*E-mail(KH): hiroi@kustro.kyoto-u.ac.jp*

## ABSTRACT

We present the first catalog of hard X-ray (4–10 keV) sources at high Galactic latitude,  $|b| > 10^\circ$ , from the first 7-months MAXI/GSC data (2009 September to 2010 March). We have developed a systematic analysis procedure to detect the faintest sources from the MAXI data, by utilizing maximum likelihood image fitting method, where the image response, background, and detailed observational conditions are taken into account. The catalog includes 140 hard X-ray sources above 7 sigma significance level.

KEY WORDS: catalogs — X-rays: galaxies — galaxies: active — MAXI: GSC

## 1. INTRODUCTION

One of the main goals of the MAXI (Matsuoka et al. 2009) mission is to provide a new X-ray catalog from the entire sky, including both transient and persistent sources. The Gas Slit Cameras (GSCs; Sugizaki et al. 2011) and the Solid-state Slit Cameras (SSCs; Tsunemi et al. 2010) cover the energy band of 2–30 keV and 0.5–12 keV, respectively, with unprecedented sensitivities as an all-sky mission. In particular, the large effective area of the GSCs at energy above 2 keV enables us to detect absorbed Active Galactic Nuclei (AGNs) that were missed in the ROSAT All Sky Survey (RASS) and will achieve a better sensitivity than Swift/BAT or INTEGRAL for moderately absorbed populations with intrinsically soft spectra.

projected images in the sky coordinates with a region size of  $11^\circ \times 11^\circ$ .

### 2.1. Searching Source Candidates

Firstly, we model the non X-ray background as a function of time, detector position, and observation conditions for each GSC camera, based on our extensive calibration of the on-board data. We then make images of the real data, model background, and their residual maps. To find source candidates, these images are smoothed with a circle of  $r = 1^\circ$ . From the integrated counts of the real data and residuals, we calculate the significance at each point as “residual / sqrt(real data)”, thus producing the significance maps (right panel of Fig. 1). We pick up signals above 4 sigma as a source candidate located at the peak position.

### 2.2. Determining Flux and Position

We perform maximum likelihood image fitting to the real image data with a model consisting of the point spread functions (PSFs) and background (Fig. 2). One complexity in the analysis of MAXI data is that the PSF is position dependent, being determined by the orbit and attitude condition. We utilize the MAXI simulator (Eguchi et al. 2009) to construct the PSF models with a sufficiently larger number of photons. In the fitting, the normalization of the PSF (i.e., flux) and its position are set to free parameters as well as the background level. We define the detection significance ( $\sigma_D$ ) as

$$\sigma_D = (\text{best-fit flux}) / (\text{its } 1\sigma \text{ statistical error}).$$

We adopt  $\sigma_D > 7$  as the detection criteria in this study, which is quite conservative, however.

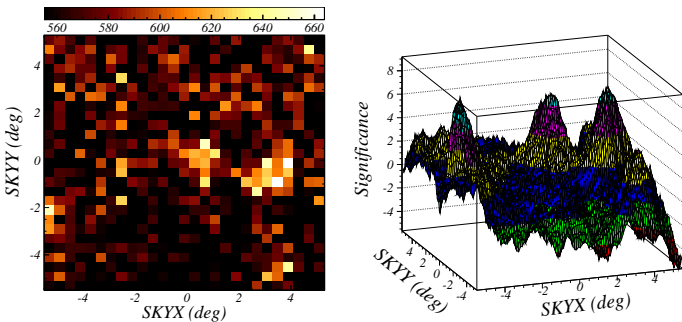


Fig. 1. An example of real data (left) and its significance map (right). We can find three source candidates in this region.

## 2. METHOD

To produce an unbiased X-ray source catalog from the MAXI/GSC data, we employ a two-step approach as described in section 2.1 and 2.2. Analysis is made for the

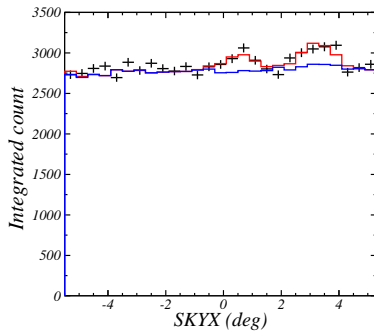


Fig. 2. Comparison of the real data (black) and the best-fit model (red: total, blue: only background). Both of these two sources have the significance of  $\sim 7\sigma_D$ .

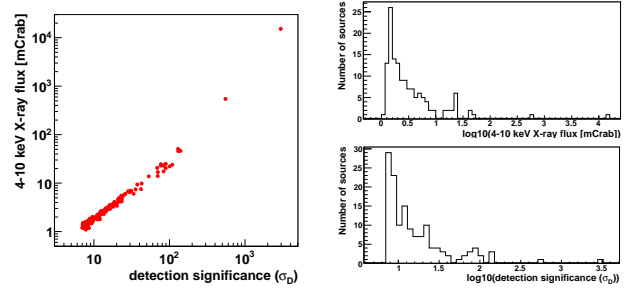


Fig. 3. Correlation between flux and detection significance (left), the distribution of flux (right top), and that of detection significance (right bottom).

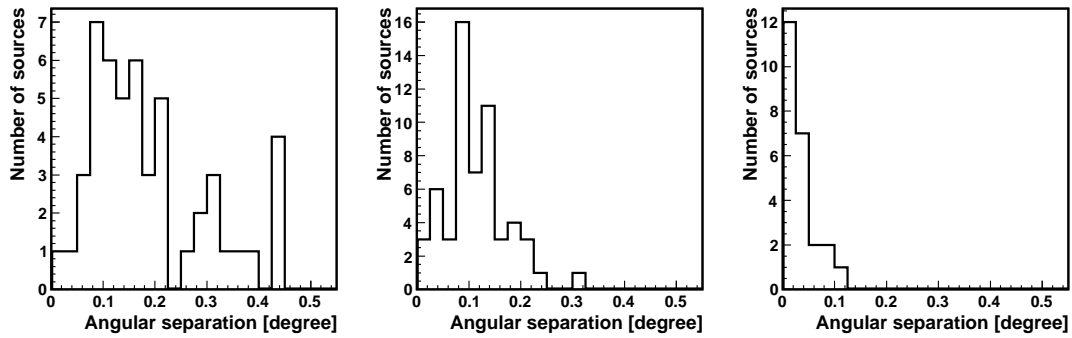


Fig. 4. Histograms of the angular separation between the MAXI position and that of the counterparts for different significance regions (from left to right,  $7-10\sigma_D$ ,  $10-30\sigma_D$ , and  $>30\sigma_D$ ).

### 3. RESULT

We detect 140 sources above  $7\sigma_D$  level in the 4–10 keV band from the high Galactic latitude sky ( $|b| > 10^\circ$ ). The properties of the cataloged sources are presented below.

#### 3.1. Flux Distribution

The plot of flux versus detection significance is shown in the left panel of Fig. 3. The limiting sensitivity is  $\sim 1$  mCrab for  $\sigma_D > 7$ , consistent with our expectation from the actual background level and observing efficiency of MAXI.

#### 3.2. Position Accuracy

Figure 4 shows the histogram of the angular separation between the MAXI position and that of the counterparts for securely identified sources. For most of the sources, the positions are typically determined within  $0.3^\circ$ . The systematic position error ( $\sigma_{\text{sys}}$ ) is estimated to be  $\sim 0.05^\circ$  from the brightest sources (right panel in Fig. 4), where the statistical errors can be ignored.

### 4. SUMMARY

From the MAXI/GSC data, we detect 140 sources above  $7\sigma_D$  level in the 4–10 keV band at high Galactic latitudes,  $|b| > 10^\circ$ , from the first 7-months data (2009 September to 2010 March). The number increases by a factor of  $\sim 2$  if we lower the significance threshold to  $5\sigma_D$ . The sensitivity limit is found to be  $\sim 1$  mCrab above  $7\sigma_D$ , consistent with an expectation from actual observing conditions of MAXI. The position accuracy is typically  $0.3^\circ$  for the faintest objects.

### REFERENCES

- Eguchi, S., et al. 2009, Astrophysics with All-Sky X-Ray Observations, Proceedings of the RIKEN Symposium, p44
- Matsuoka, M., et al. 2009, PASJ, 61, 999
- Sugizaki, M., et al. 2011, PASJ, in print
- Tsunemi, H., et al. 2010, PASJ, 62, 1371